REPORT DOCUMENTATION PAGE

Form Approved

OMB No. 0704-0188

1. REPORT DATE *(DD-MM-YYYY)* 21-07-2014	2. REPORT TYPE Final	3. DATES COVERED *(From - To)* 07-Mar-2013 to 06-Mar-2014

4. TITLE AND SUBTITLE

High Throughput Catalyst Screening via Surface Plasmon Spectroscopy

5a. CONTRACT NUMBER
FA23861314072

5b. GRANT NUMBER
Grant AOARD-134072

5c. PROGRAM ELEMENT NUMBER
61102F

6. AUTHOR(S)

Professor Paul Mulvaney

5d. PROJECT NUMBER

5e. TASK NUMBER

5f. WORK UNIT NUMBER

7. PERFORMING ORGANIZATION NAME(S) AND ADDRESS(ES)
University of Melbourne
Grattan Street
Parkville, VIC 3010
Australia

8. PERFORMING ORGANIZATION REPORT NUMBER
N/A

9. SPONSORING/MONITORING AGENCY NAME(S) AND ADDRESS(ES)

AOARD
UNIT 45002
APO AP 96338-5002

10. SPONSOR/MONITOR'S ACRONYM(S)
AFRL/AFOSR/IOA(AOARD)

11. SPONSOR/MONITOR'S REPORT NUMBER(S)
AOARD-134072

12. DISTRIBUTION/AVAILABILITY STATEMENT

Distribution A: Approved for public release. Approved for public release.

13. SUPPLEMENTARY NOTES

14. ABSTRACT
The overall goal of this research was to utilize rapid surface plasmon spectroscopy to develop a new platform to correlate catalytic performance and behavior with catalyst morphology (e.g., size, shape) of individual core/shell nanoparticles. Kinetic experiments were performed on dihydrogen adsorption, but the findings are expected to be generally relevant to other surface-critical heterogeneous chemistries. Comparative studies of $Au/TiO_2/Pt$, $Au/ZnO/Pt$, $Au/SiO_2/Pt$ were done to evaluate the spectroscopic methodology. It was found that substrate choice was critical to hydrogen adsorption and that hydrogen does not dissociate on gold nanoparticles on TiO_2 in $N_2:H_2$ mixtures, but does dissociate in air:H_2 mixtures. In the presence of Pt, dissociation occurs on Pt, and in the presence of a semiconducting matrix H_2 spillover occurs with electrons able to migrate to the gold particles. High-throughput combinatorial screening was used to create catalyst libraries by fabricating nanoarrays (20nm features) of individual nanocrystals using Capillary Force Assembly. Active research is focused on studying electron-transfer during catalysis to show that this methodology can distinguish between different individual catalysts in the array at the single nanocrystal level.

15. SUBJECT TERMS

Catalysis, Spectroscopic Techniques, nanoparticles, Morphological characterization, Defects

16. SECURITY CLASSIFICATION OF:			17. LIMITATION OF ABSTRACT	18. NUMBER OF PAGES	19a. NAME OF RESPONSIBLE PERSON Kenneth Caster, Ph.D.
a. REPORT	b. ABSTRACT	c. THIS PAGE	UU	17	
U	U	U			19b. TELEPHONE NUMBER *(Include area code)* +81-3-5410-4409

Standard Form 298 (Rev. 8/98)
Prescribed by ANSI Std. Z39.18

<div align="center">

Final Report for AOARD Grant 134016

FA2386-13-1-4072

"**High Throughput Spectroscopic Catalyst Screening by Surface Plasmon Spectroscopy**"

Date 10th May, 2014.

</div>

PI information: Paul Mulvaney; mulvaney@unimelb.edu.au; University of Melbourne; School of Chemistry & Bio21 Institute; Level 2 Nth, 30 Flemington Rd., Parkville, VIC., 3010, Victoria Australia, Tel: +61 3 8344 2405; Fax: +61 3 93481595.

Period of Performance: April 1, 2013 - March 31, 2014.

Specific Aims from original AOARD Application:
- Develop a new experimental technique for studying important chemical reactions such as CO oxidation, H_2 production and other surface catalysed reactions.
- Provide experimental proof that catalysis can be monitored at the single particle level.
- Prove that spectroscopy can provide fast reliable screening of catalysts at the ensemble and single particle level.
- Provide evidence that SPS can be used to identify the key facets in important catalytic reactions. This data can be directly correlated to DFT calculations of the binding energies of substrates such as CO, O_2 and CO_2 to different crystal facets.

Abstract:
Why the work was done: Catalysts play an essential role in commercial chemistry, contributing directly to some 75% of all products in the petroleum industry and generating some $900 billion dollars in products annually around the world, while employing (in 1990) 750,000 workers. In the longer term, breakthroughs in catalysis are essential for solving several global problems. For example, to alleviate long-term climate change, catalysts for CO_2 reduction are needed, while cheaper ammonia through catalytic N_2 fixation offers cheaper fertilisers. Furthermore 70% of human energy consumption is in the form of fossil fuels, and in order to meet renewable energy targets, cheap catalysts for solar driven water splitting into hydrogen and oxygen are required.

Central to all these global challenges is the need for better understanding of how catalysts work. In this 1-year study, we have developed a new platform for studying catalysts spectroscopically. The goals are to show that cataysts undergo spectroscopic changes during reactions that allow new insights into how they work. We are also working on methods to enable this technique to enable high throughput testing of catalysts.

What was accomplished: In the 12 month period, we have:
   (i)   Constructed a new spectroscopic method for studying electron transfer during catalysis and shown that this spectroscopic method can distinguish different catalysts. We also find we can directly investigate the role of different support materials.
   (ii)   Created a nanofabrication method to allow us to create a library of single nanoparticles so that we can investigate the catalytic efficiency of materials at the single nanocrystal level.

Background & Concept:
A heterogeneous redox catalyst can be envisaged to work as follows. The reducing agent adsorbs to the catalyst, and usually it disociates, which leads to formation of reactive surface intermediates.

<div align="center">1</div>

Electrons are transferred from the intermediates to the metal, which can store large numbers of charges. These are picked up by the oxidant leading to reduction. Key questions in catalysis are always: (i) what is the best metal (ii) what role does the matrix play (iii) how are charged species stabilized?

$$D^- + A \Longleftrightarrow D + A^-$$

$$DH_2 + A \Longleftrightarrow D + AH_2$$
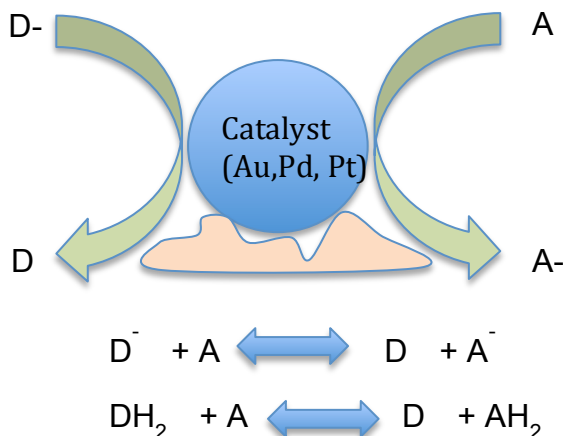
Scheme 1: Redox catalysis involves electron exchange or transfer from a donor D- to an acceptor A. The metal accelerates the chemical reaction by allowing large numbers of electrons to collect, acting like an "electron pool". In "real" reactions, protons are always intricately involved and the reaction is usually a multiple H atom transfer from DH_2 to A. Understanding where the protons reside and how coupled transfer of protons and electrons proceeds is at the heart of redox catalysis.

In normal catalysis, the focus is on measuring the ***global*** rates of reaction as a function of the reactant concentration and products are analysed by GC etc. However this provides little insight into the mechanism. By looking at changes in catalyst charge, we aim to uncover more details about mechanisms. In Scheme 1, we highlight how simple redox catalysis works. The first question is, does a reductant transfer electrons to the catalyst even when the acceptor is not present? Because we can see the catalyst particle accumulating or losing charge, we can simplify the redox chemistry: By exposing the catalyst just to the reductant D- (in this case H_2 or CO), we can see the "half-cell" reaction:

$$D\text{-} \; + \; Catalyst \; \Leftrightarrow D + (Catalyst)^-$$
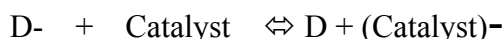
In this AOARD project we found that we can clearly see large differences, depending on whether there is oxygen or nitrogen present, the nature of the substrate and the presence of other catalyst particles in the system.

Experiment:
I. Instrumental Set-Up: AOARD funds were used primarily to purchase a new Princeton Instruments Isoplane spectrometer with improved optics for the dark field system. This new instrument enables broad spectra to be collected faster, with higher wavelength resolution and without manual stitching. Our spectroscopy system was also modified to enable gas studies.
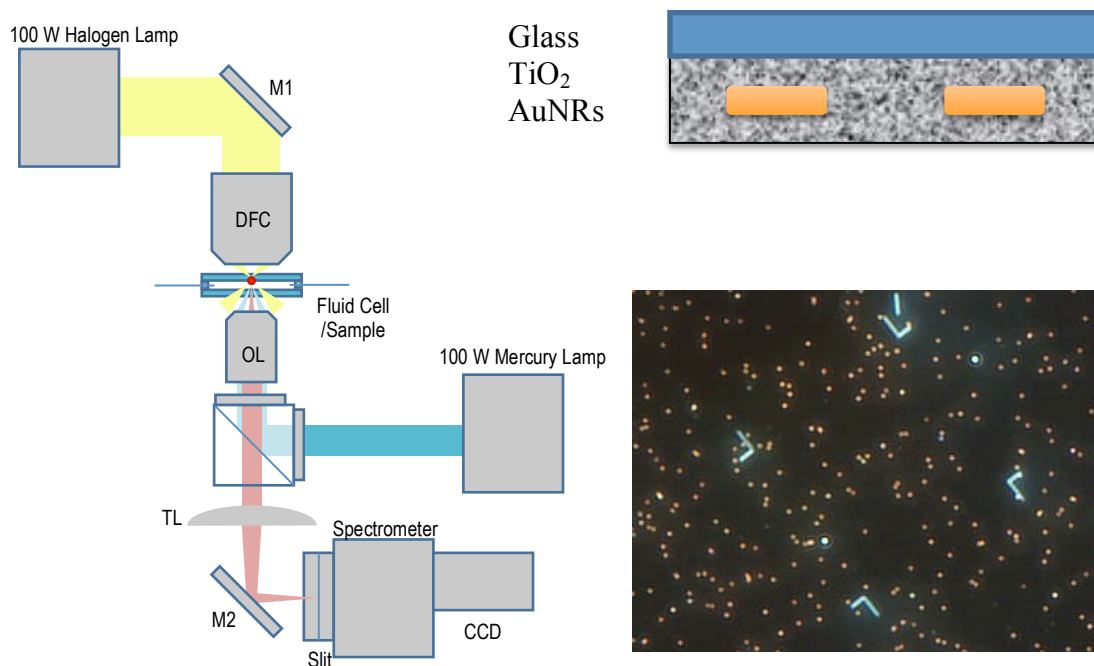
Scheme 1: A dark field spectroscopy set-up was constructed with a home-built fluid cell so that we can study the optical properties of single catalyst particles in the presence of different gases. **Left:** The experimental set-up. Light from either a mercury lamp or from a halogen lamp illuminates the microscope slide through a dark field condenser. Light scattered by single particles is collected by a spectrometer and into a CCD. **Bottom right**: A dark field image showing a hundred or so single, well-dispersed gold nanocrystals. We use a FIB to mark the microscope grid (blue lines) so we can locate repeatedly the same single nanoparticle in the SEM, allowing us to compare the spectral results with morphology. **Top Right**: The catalysts can be dispersed onto glass or within various oxide matrices (e.g. ZnO, silica, titania) as long as they do not scatter light.

II. Preparation of Catalyst Particles and Substrates:

   (a) **Gold NRs,** with 13±4nm diameter and 40±9nm length, were prepared according to the seed-mediated method proposed by El-Sayed, by reducing $HAuCl_4$ with sodium borohydride ($NaBH_4$) in water, in the presence of hexadecyltrimethylammonium bromide (CTAB) to obtain the seeds. A growth solution was then prepared with CTAB as templating agent for the NR growth and ascorbic acid as a mild reducing agent; the final step was the addition of 12 μL of seed solution to the growth solution at 27-30 °C. The color of the solution gradually changed within 30 min. In order to eliminate CTAB in excess the NRs has been centrifuged twice at 7000 rpm for 20 min, and redispersed in water each time. The final solution was diluted 10 times from the as-synthesized concentration.

   (b) Platinum colloids with 10 nm diameter were prepared using the polyol method. A solution containing 80 mM chloroplatinic acid hydrate (H_2PtCl_6) in ethylene glycol was rapidly added to a solution of poly(vinyl pyrrolidone) (PVP) 30 mM and sodium nitrate ($NaNO_3$) with ratio $NaNO_3$/ H_2PtCl_6 9:1 in ethylene glycol, at 160 °C. Ethylene glycol serves as both the solvent and the reducing ag

3

ent. The NPs were dispersed in ethanol leading to a 30 mM sol.

(c) **TiO₂ NPs** were synthesized by adding 10.5 mmol of titanium tetraisopropoxide (Ti(OPr)$_4$) into a previously prepared solution containing water, hydrochloric acid and methanol with molar ratios H$_2$O/TiOPr=12.25, HCl/ TiOPr=1.72. The solution was stirred for 60 min utes at room temperature and then heated in an oil bath at 70 °C for four hours under reflux. Particles were then precipitated and dispersed in methanol to yield a clear TiO$_2$ anatase sol.

(d) **SiO₂ NPs:** A silica sol was prepared starting from tetraethyl orthosilicate (Si(OC$_2$H$_5$)$_4$, TEO S), ethanol, water and hydrochloric acid using the following molar ratios: H$_2$O/TEOS = 4, EtOH / TEOS = 2, HCl/TEOS=0.01. The solution was left to stir at room temperature for 1 hour before deposition.

III. Sample Preparation: Samples for DFM measurements were deposited on fused silica quartz slides or silicon substrates by spin coating at 3000 rpm for 30 s and annealed for 10 min in air. The prepared samples are reported in Table 1. The bare Au NR samples (1) were prepared by spin coating the aqueous Au colloid solution at 3000 rpm for 30 s and then drying the sample at 70 °C for 10 min. The Au NRs + Pt NPs samples (2) were prepared by spin coating the Pt NPs containing ethanol solution at 3000 rpm for 30 s and dried at 150 °C. Following this, the aqueous solution of Au NRs was spin coated onto the Pt NPs monolayer in the same manner as the bare Au NR samples, and annealed at 70 °C. The Pt NPs were deposited at the bottom because they need to be annealed at a higher temperature to work effectively as a catalyst and on the other hand, the Au NRs cannot be treated at temperatures higher than 70-80 °C as they tend to spheroidize; this restriction determined the order of the layers in the case of bare NPs. This restriction was overcome by covering the NRs with the TiO$_2$ matrix, as this enables the annealing temperature to be increased up to 150°C without changes to the NR morphology. The Au NRs + TiO$_2$ samples (3) were prepared initially in the same way as the Au NR sample, with a further layer of TiO$_2$ NPs deposited at 3000 rpm for 30 s and then annealed at 150 °C for 10 min. The Au NR + (TiO$_2$-8%Pt NP) samples (4) were prepared in the same way as the previous sample, except with a ethanolic mixture of TiO$_2$ and Pt NPs in a ethanolic solution instead of just TiO$_2$. Au NR + TiO$_2$ + Pt NP samples (5) were prepared exactly as the Au NR + TiO$_2$ samples were, except before the annealing step, a sub-monolayer of Pt NPs were spin coated on the top of the sample. Finally, the Au NR + (SiO$_2$-8%Pt NP) sample (6) was prepared by spin coating the Au NR solution as for the bare Au NRs, then, the SiO$_2$ solution was mixed with the Pt NP solution, and spin coated onto the top of the

4

Au NR sub-monolayer. These samples were also annealed at 150 °C for 10 min.

IV. Instrumentation: Absorption spectra were collected with an Agilent 8453 UV-visible spectrometer, between 200-900 nm, on films deposited on glass substrates. X-ray diffraction (XRD) characterization has been performed by using a Philips PW1710 diffractometer on films deposited on Si substrates. The analyses were performed at an incident angle of 3° using CuKNi-filtered radiation at 30 kV and 40 mA. Optical constants n and k and films thickness were evaluated by measuring variables Ψ and Δ with a J.A.Wollam V-VASE spectroscopic Ellipsometer at two angle of incidence (60° and 70°) in the wavelength range of 300-1500 nm. This data was fitted using WVASE ellipsometry software. Transmission electron microscopy (TEM) images were acquired on a FEI Technai TF20 microscope operating at 200 kV. TEM samples were prepared by drop casting the sample solutions onto copper TEM grids (300 carbon mesh) and drying in ambient conditions. Scanning electron microscopy (SEM) was performed on a FEI Nova 200 Nanolab microscope operating at 5 kV. The single-particle time-resolved measurements were performed using a Nikon TE2000-S Eclipse Inverted Microscope equipped with a Nikon dry dark-field condenser and a 40X/0.6 NA ELWD dry objective lens in transmission configuration (see Scheme 1). An Isoplane SCT 320 imaging spectrograph (Princeton Instruments) fitted with a PIXIS 1024F CCD detector was coupled to the image output of the microscope for spectroscopic measurements. The samples were placed in a custom made cell which allow scattering spectra to be collected under different environments. The measurements were taken at room temperature (RT) using 50,000 ppm H_2, balanced with N_2 or air, with a flow rate of 0.07 L/min.

Results and Discussion:
I. Hydrogen Interaction with Gold Nanocrystals on Glass

We first tested the stability of the spectroscopic system and the Isoplane spectrometer. When gold spheres or rods are exposed to nitrogen gas, the scattering spectra are found to be extremely constant. We find that the experimental peak position can be determined to better than ±1nm for minutes at a time. We use IGOR to fit the spectral peak position, intensity and FWHM numerically (see Appendix). There is little evidence for heating effects and the biggest challenge is slow drift in the focal position of the microscope. The control experiments show that surface plasmon spectroscopy of single particles in the absence of any surface chemical process provides is very stable.

In Figure 1, we show the first key results of this work. It has long been claimed that gold is a

5

poor catalyst for hydrogenation because it does not form stable bonds with surface H atoms. H atons are strong reductants and if H_2 dissociates on gold, it should inject electrons leading to a blue shift in the scattering spectra. In Figure 1, we show the effect of exposing bare gold nanorods (NR) initially under dry nitrogen to 5% H_2. It can be seen that alternate injections of hydrogen and nitrogen lead to no discernible spectral changes to the catalyst. In agreement with literature, we do not see any evidence for hydrogen dissociation on gold nanocrystals.
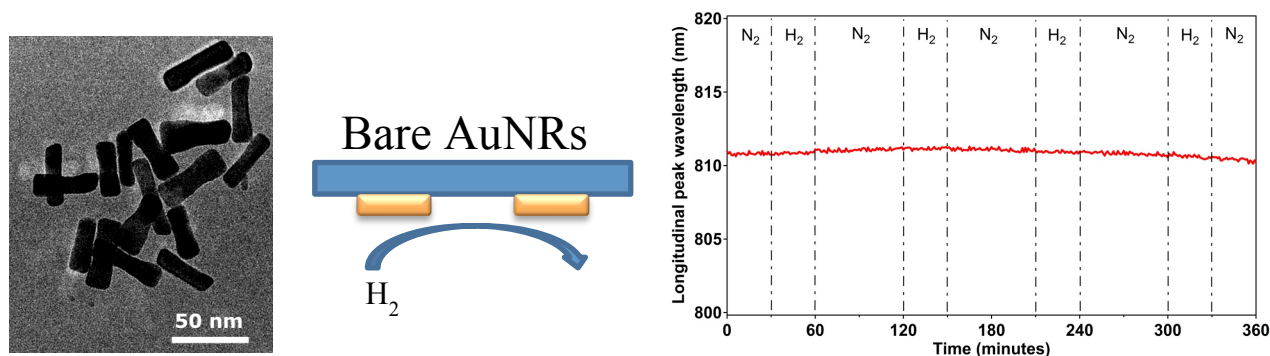
Figure 1: Bare gold nanorods were dispersed on glass microscope slides. They were exposed to N_2 first and the spectra were found to be extremely stable. They were then exposed to cycles of N_2, followed by 5% H_2 in N_2. There was no discernible change in position, showing that H_2 does not adsorb significantly to gold rods at room temperature.
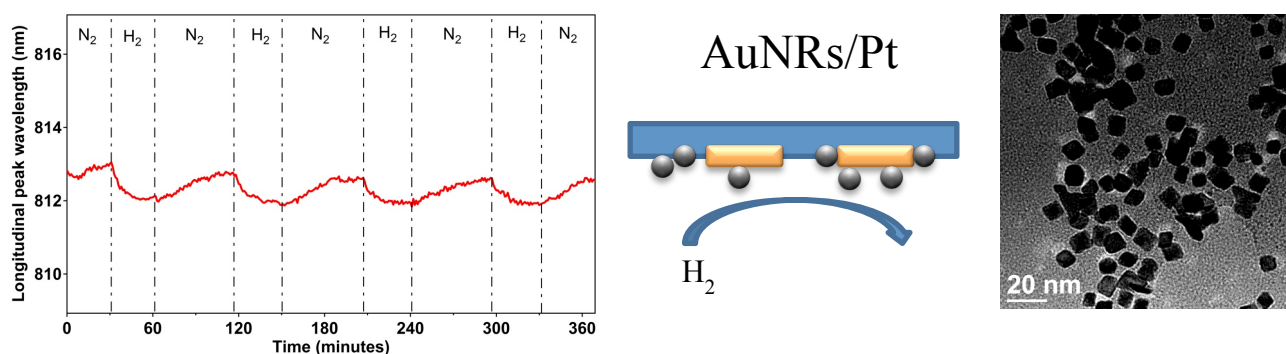

Figure 2: When a small amount of Pt nanocrystals were spin coated onto the slide, the scattering spectra from the **GOLD NRs** did shift weakly to the blue, showing that the gold particles accumulated electrons under these conditions.

However, when a small concentration of platinum nanoparticles is adsorbed onto the gold particles, and the sample exposed to 5% H_2 in N_2, small clear blue-shifts are observed (Fig 2). We can explain this shift by assuming that H_2 dissociates on the Pt particles and that free electrons then migrate to the gold particles. Noble metals should act as a sink for electrons. In this case, the gold particles really act as a spectroscopic sensor, not a catalyst. They are charged only when the Pt nanocrystals are active. Our initial conclusion from this is that the literature is completely correct. Gold by itself is unable to function as a

6

hydrogenation catalyst. The question that arises is, do the Pt particles need to be touching the gold particles for electron transfer to occur or can the electrons be transported to the gold through the substrate?

II. Effect of TiO$_2$ Substrates

To determine whether electrons migrate through a substrate during catalysis or are localised to one nanocrystal, we compared three substrates: TiO$_2$, ZnO and SiO$_2$. In Figure 3 (left), we present the time dependent peak position of the gold nanorod spectrum vs time during exposure to N$_2$:H$_2$ cycles. As before, there was no discernible effect of hydrogen and we conclude that there is no adsorption of hydrogen onto gold irrespective of whether it is supported on glass or titania.
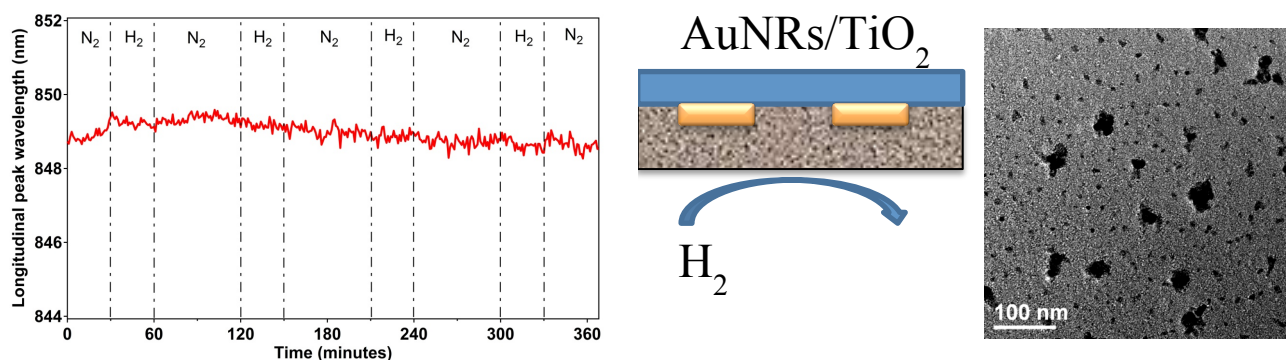

Figure 3: (Left) Plot of the surface plasmon peak of gold nanorods embedded in TiO$_2$ sol-gel films as a function of time during cycling with nitrogen and 5% H$_2$:N$_2$. (Right): Pt particles dispersed into the TiO$_2$ films.
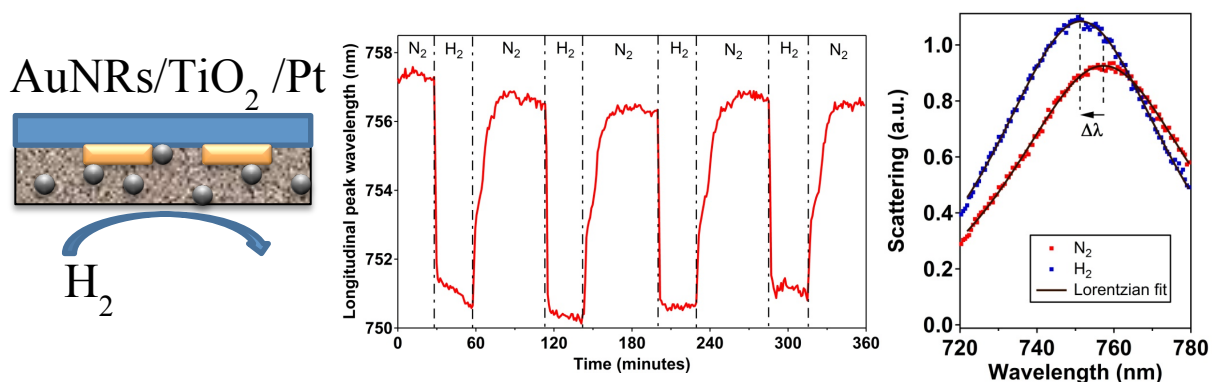

Figure 4: (Left and Middle): Effect of Pt particles on the surface plasmon peak during N$_2$:H$_2$ cycling at room temperature. (Right): Typical single particle spectrum before and during H$_2$ exposure showing magnitude of the blue-shift. Note the increase in scattering cross section. Each curve of 80 data points has been fitted with a Lorentzian curve.

We then introduced Pt particles into the titania solution during spin coating. An SEM of the Pt particles in the film shows they were well dispersed with a few aggregates.

7

Remarkably, we immediately see strong, very reversible shifts in the peak during cycling (Figure 4). There is also an increase in scattering cross section of the particles during catalysis. Typically, the peaks shift within 30sec to 1 minute of exposure. From this we conclude that only in the presence of Pt does the gold exhibit a blue-shift. It appears gold is a spectator during Pt interactions with hydrogen gas. What we see here is often termed "hydrogen spillover". Electrons or H atoms migrate from catalytically active Pt to the gold, but it is unclear still whether the Pt particles need to be in direct contact with gold. In other words are the only gold particles picking up electrons, those in direct contact to a Pt particle? To answer this question, we need to physically isolate the Pt and gold particles and determine whether electrons still accumulate on the gold particles.
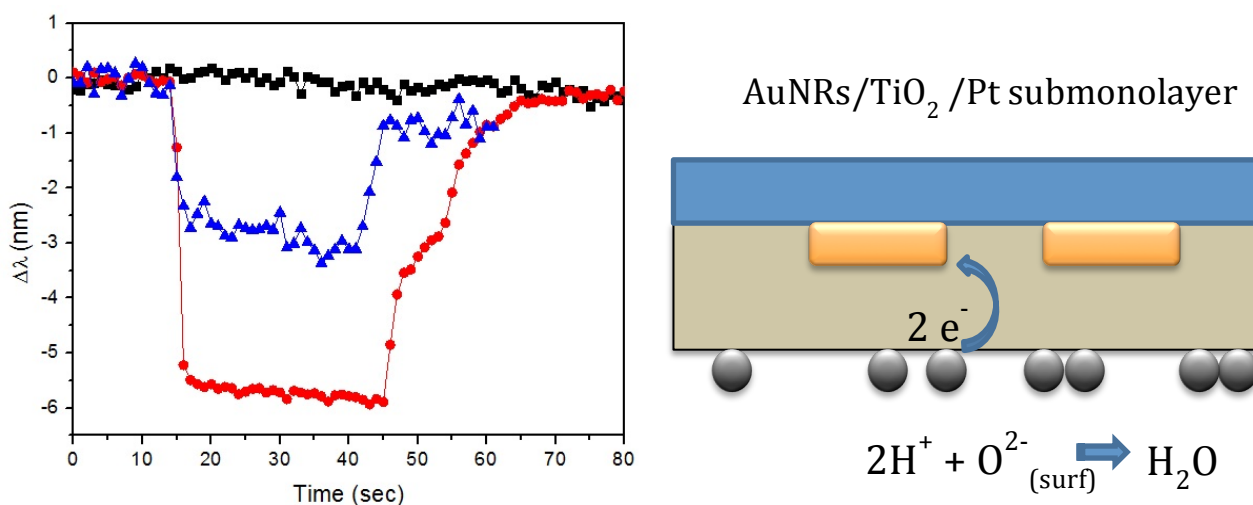

Figure 5: Pt particles are spin-coated on top of a gold-TiO_2 film and exposed to H_2. **Left**: Spectral shifts for gold NRs in the absence of Pt particles (black), in the presence of Pt particles within the matrix (red) and when only on top of the titania film (blue). Cycles are N_2 followed by 5% H_2 in N_2.

In Figure 5, we isolated the gold nanoparticles from the Pt particles with a titania film. The gold NRs still exhibit a spectral blue-shift. This means that electrons liberated on Pt do migrate through the substrate. These results lead to the surprising conclusion that catalyst particles directly commmunicate with each other during catalysis. Electrons flow from metal particle to metal particle through the substrate, at least for titania, a semiconductor, widely used in catalysis.

8

III. Role of the Substrate: We also compared spin coated sol-gel films of ZnO and SiO$_2$ to determine how important the carrier substrate is.
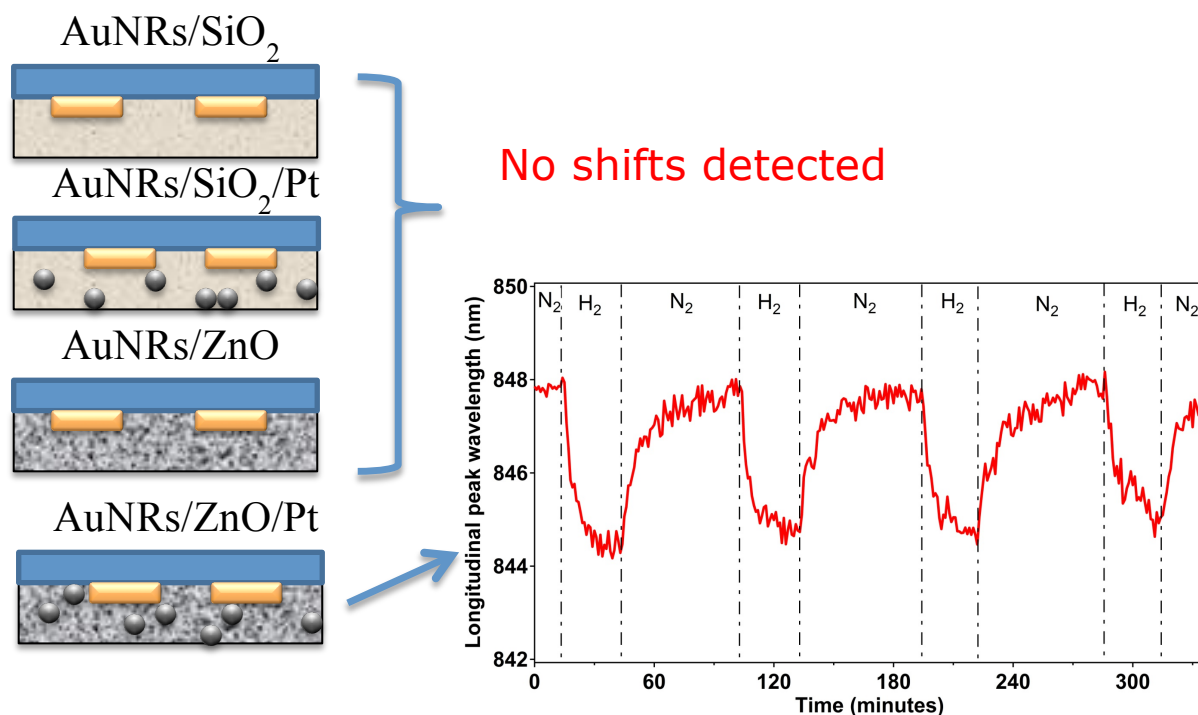

Figure 6: Other key results. When gold rods were immersed in silica sol-gel substrates or ZnO, no shifts were observed. When Pt particles were embedded in silica, no shift was obs erved. However, when Pt particles were embedded in ZnO, small blue-shifts were observed.

The crucial role of the substrate is apparent from the results in Figure 6. Silica is a poor substrate for hydrogen dissociation. No shifts are observed even when Pt particles are embedded in the silica. However Au NRs embedded in ZnO containing Pt particles do exhibit a blue-shift, although they are inert in the absence of Pt. This demonstrates that the substrate needs to be semi-conducting. Insulating oxides such as SiO$_2$ cannot facilitate electron transfer from the Pt to gold particles. Below we pictorially summarise how we have tried to use surface plasmon spectroscopy to study H$_2$ interactions with gold particles. Most importantly from this part of the study, we find that the substrate is crucial and that electrons migrate through the substrate. We do not know how much of the hydrogen on Pt dissociates into free electrons and how much remains as H atoms on the Pt surface. An important trend is shown in Figure 7 below. When Pt particles are adsorbed directly onto the gold NRs, the shifts are smaller than when they are dispersed into an overlying TiO$_2$ substrate. There is a faster and more extensive dissociation in the latter case. Hence, we deduce that the factor limiting the rate of H$_2$ dissociation is not electron transfer to the matrix but the availability of H+ binding sites. Only when there is a good metal oxide to

9

soak up the protons producued during electron injection can free electrons be generated. TiO_2 is a better substrate because it is a better host for protons than ZnO or SiO_2, which are more acidic surfaces.
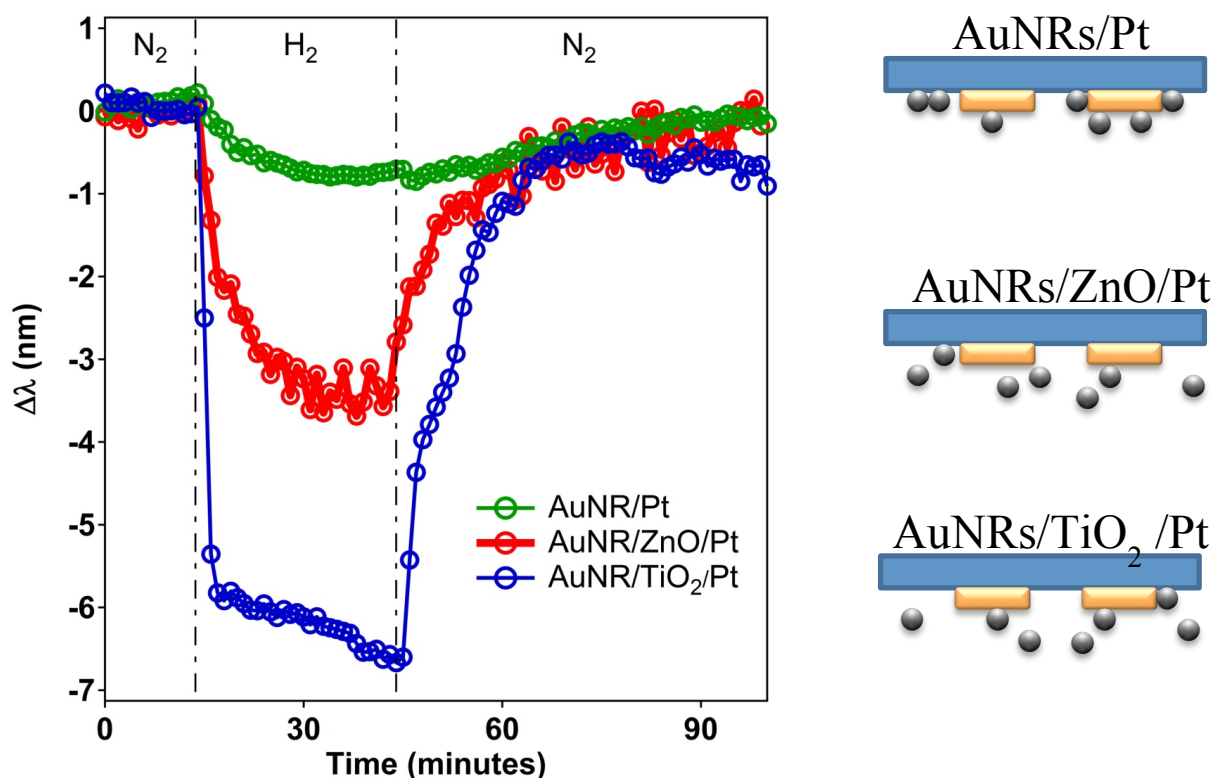

Figure 7: Comparing typical traces for the shift of the SP band of gold during catalysis leads to the conclusion that the preseince of TiO_2 leads to faster and more extensive hydro gen dissociation. The gold here is simply acting as an indicator for the availability of free electrons in the system during hydrogen gas exposure.

V. The Role of Oxygen

For most of this 1-year study, experiments were carried out on N_2:H_2 mixtures. N_2 was used primarily to keep out moisture and also to minimize the risks of explosion due to having O_2:H_2 mixtures in the lab. All the results so far are consistent with literature, which claim that hydrogen does not dissociate at room temperature on gold metal surfaces, even for 30nm rods and spheres. We then explored the behaviour of using air:H_2 mixtures rather than N_2:H_2. The results were completely unexpected.

When air was used as the reference gas, introduction of hydrogen led to blue-shifts for Gold on titania (in the absence of Pt). This was the first time we had seen clear electron accumulation on gold in the absence of Pt.
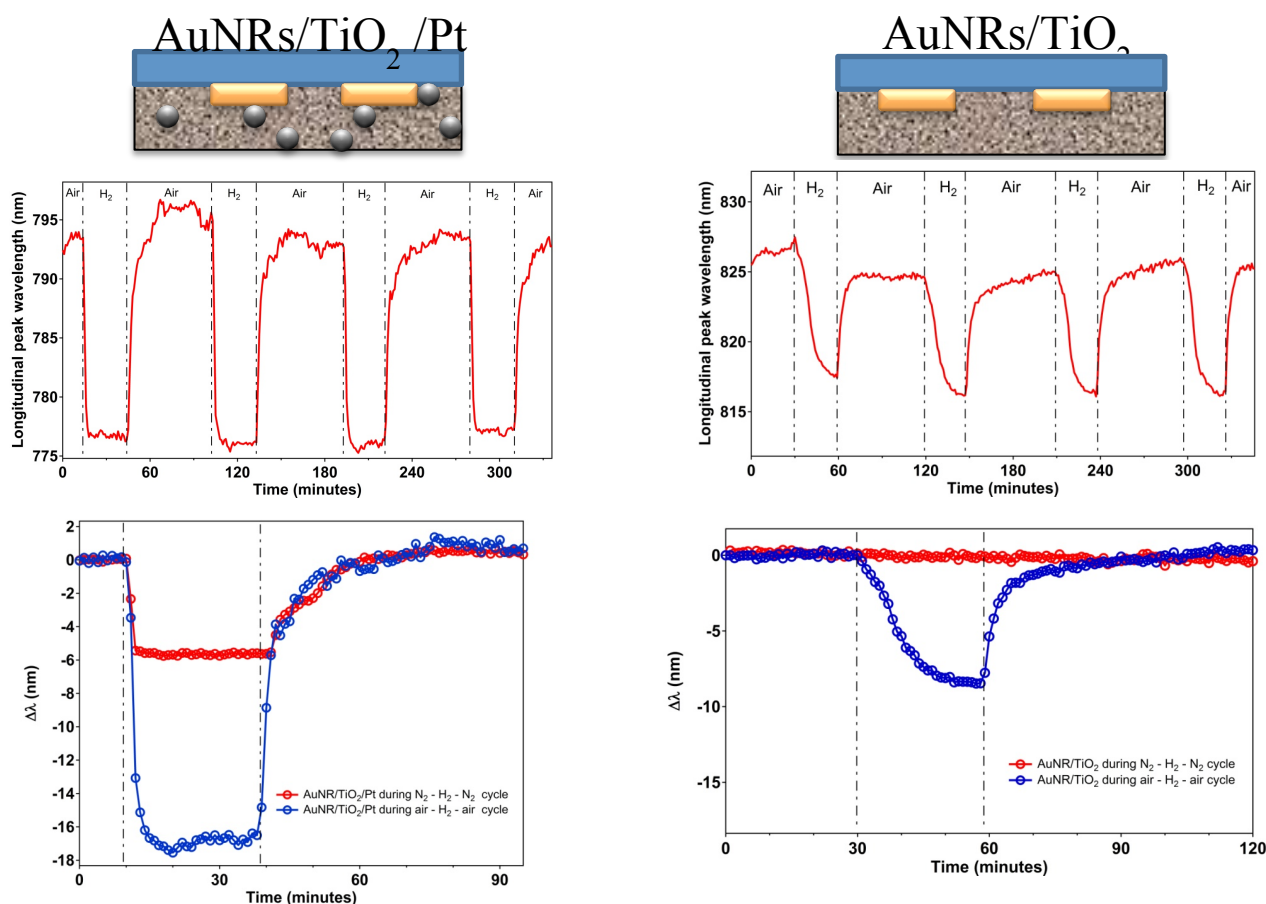
10

Figure 8: The role of Oxygen. When the buffer gas is switched from N_2 to air, gold nanocrystals are switched on! (Right): The gold rods now exhibit a clear and strong blue-shift upon exposure to air. We observe the first clear evidence for room temperature a dsorption of hydrogen onto gold nanorod surfaces. (Left): Pt still has a pronounced role. The blue-shifts become even stronger showing that in the presence of air and Pt NCs, accumulation of electrons is even stronger on the gold catalyst surfaces.

The role of oxygen is surprising. Why would electron transfer to gold be enhanced by an oxidant, which removes electrons from the noble metal surface?

The clue lies in the fact that again, gold nanorods show no shift in air when adsorbed to silica substrates. This suggests that it is the interaction of oxygen with the TiO_2 which is critical. We deduce that oxygen creates proton acceptor sites on TiO_2. In order to dissociate into electrons and protons, the protons must also adsorb to the catalyst surface. Oxide ions on the surface play a crucial role. Protons bind to surface oxides and form wat er, releasing electrons into the substrate.

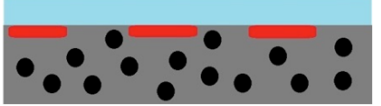$$H_2 \rightarrow 2H^+ + 2e^- + O^{2-}(ads) \rightarrow H_2O + 2e^-$$
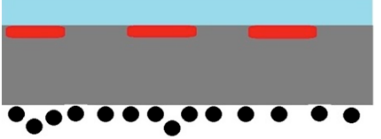
11
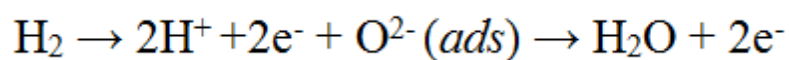
The capacity of the substrate to soak up protons determines the amount of H_2 dissociation and electron harvesting by the gold surface. We still cannot determine wther the H_2 dissociates on the gold, with the protons migrating to nearby TiO_2, or whether the H_2 dissociates onto the TiO_2 itself with free electrons wandering through the TiO_2 and simply being trapped on the gold particles.

Below we summarize the way we have tried to uncover the interactions of hydrogen with gold nanocrystal surfaces. We believe the results here demonstrate that surface plasmon spectroscopy offers an important new technique for probing the mechanisms involved in rediox catalysis.

Matrix Effects:
Table 1- The order of the layers and the material composition for the six different samples prepared for optical measurements, in red the Au NRs, in black the Pt NPs, in gray the TiO_2 matrix and in blue the SiO_2 matrix.

	Sample	Composition	
1	Au NRs	Bare Au NRs on glass	
2	Au NRs + Pt NPs	Au NRs and Pt NPs on glass	
3	Au NRs + TiO_2	Au NRs on glass covered with TiO_2 film	
4	Au NRs + (TiO_2-8%Pt NPs)	Au NRs on glass covered with TiO_2 film containing Pt NPs	
5	Au NRs + TiO_2 + Pt NPs	Au NRs on glass covered with TiO_2 film on top of which Pt NPs have been deposited	
6	Au NRs + (SiO_2-8%Pt NPs)	Au NRs on glass covered with SiO_2 film containing Pt NPs	

Summary Part I.
Using hydrogen adsorption as a simple system, we have shown that:

- Gold particles interact strongly with the environment and substrate. The best system is gold and titania, gold on ZnO works less effectively, while gold on silica does not function as a catalyst.

- Hydrogen does not dissociate on gold nanoaprticles on TiO_2 in N_2:H_2 mixtures. However, it does dissociate in air:H_2 mixtures.

- In the presence of Pt, dissociation occurs n Pt and in the presence of a semiconducting matrix, H_2 spillover occurs with electrons able to migrate to the gold particles.

12

- Generally adsorption is reversible but equilibrium takes several minutes at room temperature.

In the study to date, the results have focussed more on "yes" or "no" questions. In future studies we will attempt to do quantitative studies of adsorption kinetics etc.

We will then shift to looking at CO, for which gold is a known catalyst and try to see if morphology differences can be discerned.

II. Fabricating Arrays for High Throughput Analysis

The second part of our program has been the design of nanofabricated arrays to streamline and accelerate optimization of catalysts. We use a combination of nanofabrication to produce PMMA templates with customized cavities of various shapes and sizes (see Figure 9). We then introduce a heterogeneous mixture of gold nanoparticles with different morphologies and use Capillary Force Assembly (CFA) to push indiviudal particles into the array (see Figure 10). The array allows us to automate the study of catalysis and to address and locate or re-locate the same particle multiple times. The hope is that we will see differences in the spectra as we expose these arrays to different reactants. This work is ongoing.
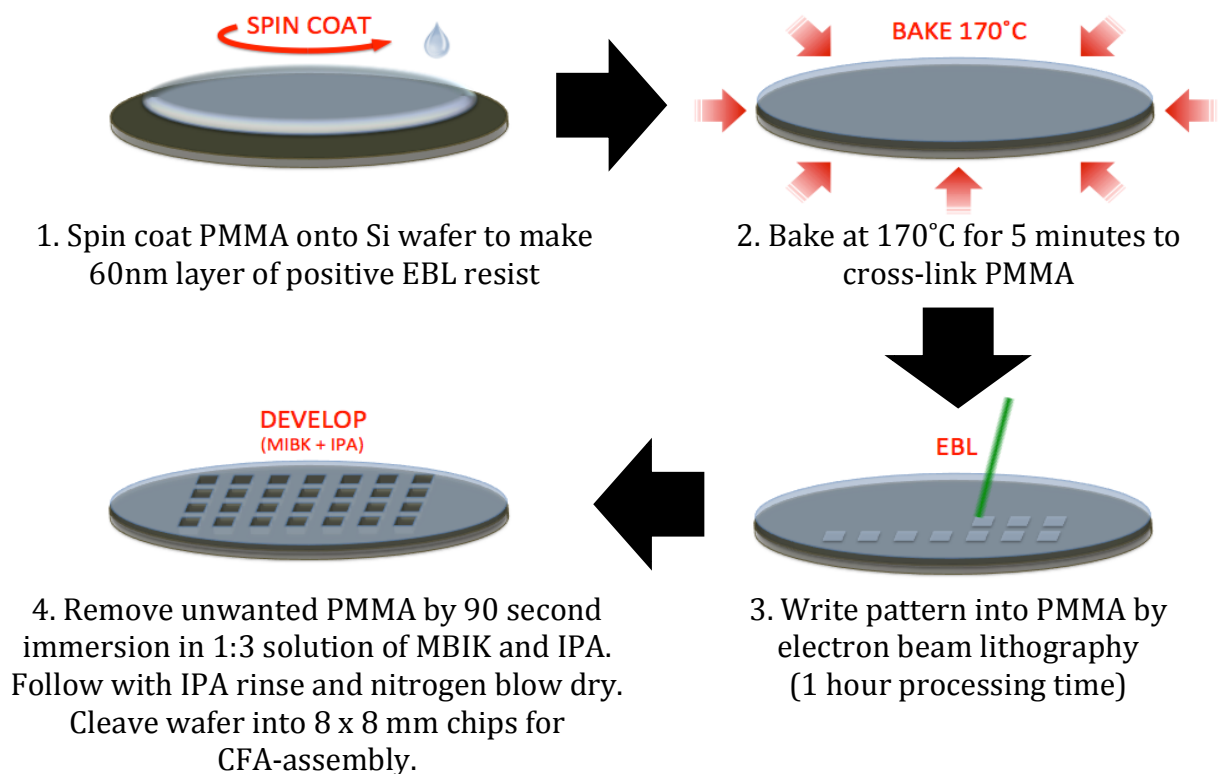

1. Spin coat PMMA onto Si wafer to make 60nm layer of positive EBL resist

2. Bake at 170°C for 5 minutes to cross-link PMMA

4. Remove unwanted PMMA by 90 second immersion in 1:3 solution of MBIK and IPA. Follow with IPA rinse and nitrogen blow dry. Cleave wafer into 8 x 8 mm chips for CFA-assembly.

3. Write pattern into PMMA by electron beam lithography (1 hour processing time)

Figure 9: Nanofabrication route for printing 20nm features on silicon wafers for assembly of single metal nanoparticles.

13

Having metal particles in an array helps us do multiple experiments on single particles and we can alwys do SEM after to look for morphology changes.

It had previously been shown that gold spheres down to 50nm could be captured in these cavities using CFA. We want to extend this down to 20nm and capture a wide range of particle shapes in one array.

The major challenge has been controlling the contact angle of the nanoparticle solutions. CFA works only if the contact angle of the solution on the substrate is maintained around 45 degrees. However, the surfactants used to control the particle shape (typically a cationic surfactant such as CTAB) also reduce the contact angle and the particles do not get trapped. However removal of the surfactant lads to particle aggregation so we are working on this aspect at present.
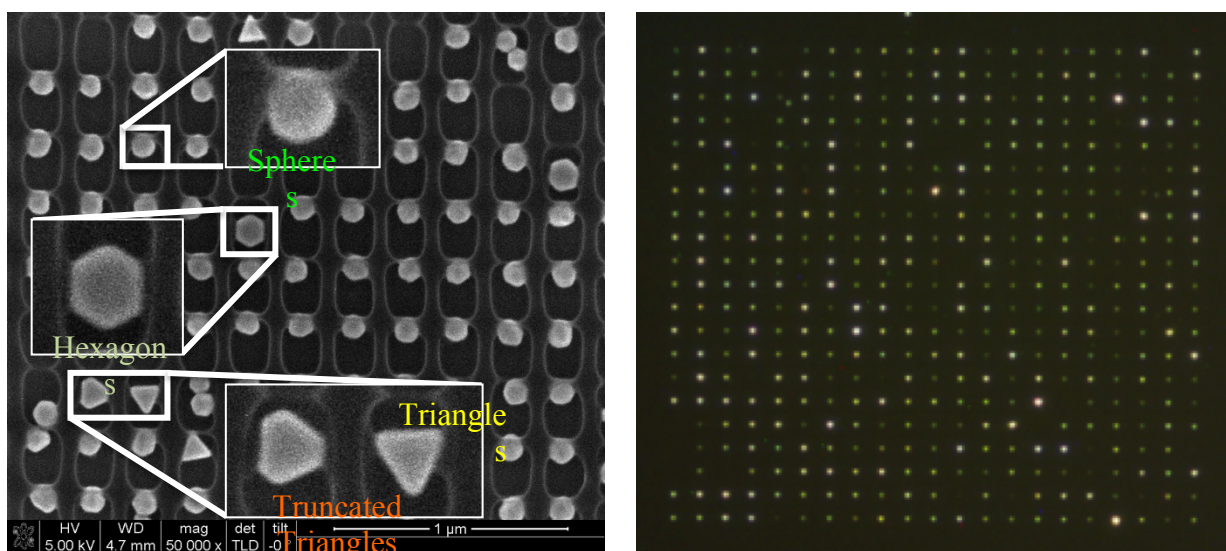

Figure 10: (Left): SEM images of single gold paricles including spheres, triangular prisms, hexagonal plates and rods in close packed PMMA cavities. For Dark Field Spectroscopy, the particles must be > 5 microns apart to stop overlap of the spectra. (Right): Optical image of well dispersed single gold particles in a PMMA array. The particles are mostly spheres with some triangular prisms and a small perentage of rods.

Summary:
Our second goal of creating arrays of assembled nanoparticles for screening is working. We have managed to create a few arrays that work as shown in Figure 10, but it is not yet routine. We have found EBL expensive and there is a lot of down time. We are working on switching to using NanoImprint Lithography (NIL). In this process a single master is used to stamp replicate array structures into a polymer. This has worked several times, although our small feature size pushes NIL to its limits. Adhesion of the Master is an issue as well as clean cavity shape. Nevertheless we feel we are close to making this a via platform for catalyst screening.

Appendix:
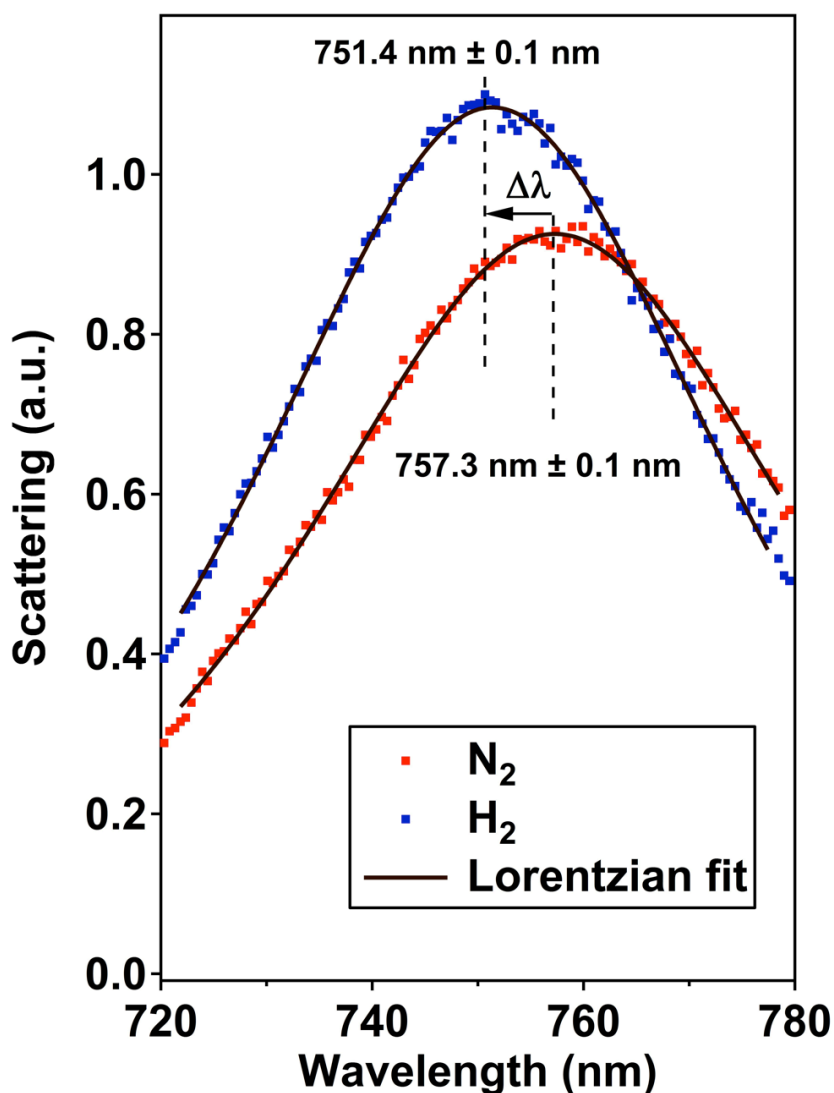
Figure S1: Typical scattering spectra. Using Igor, a Lorentzian fit is used to give the least squares fit to the peak position. Typical accuracy is ±0.5nm for a 140-point spectrum. It takes about 1 minute to fit 400 such spectra and to plot the peak position vs time. However, downloading the files from the spectrometer takes much longer. Hence fits are done after the experiment, not in real time. This means we only discover flawed experiments after completion.

Sample	Thickness (nm)	Refractive index n (at 632 nm)
TiO_2	42	1.89
SiO_2	100	1.43

Table S2- Thickness and refractive index values of the layers used for coating the Au NRs measured by ellipsometry. Effect of Catalysis on Refractive Index: One unexpected effect is that hydroen incorporation into the TiO2 matrix can alter the refractive index of the substrate. This effect can on its own give rise to a small spectral shift in the surface plasmon resonance. However simulations with the data below show this cannot account for the observations we see.
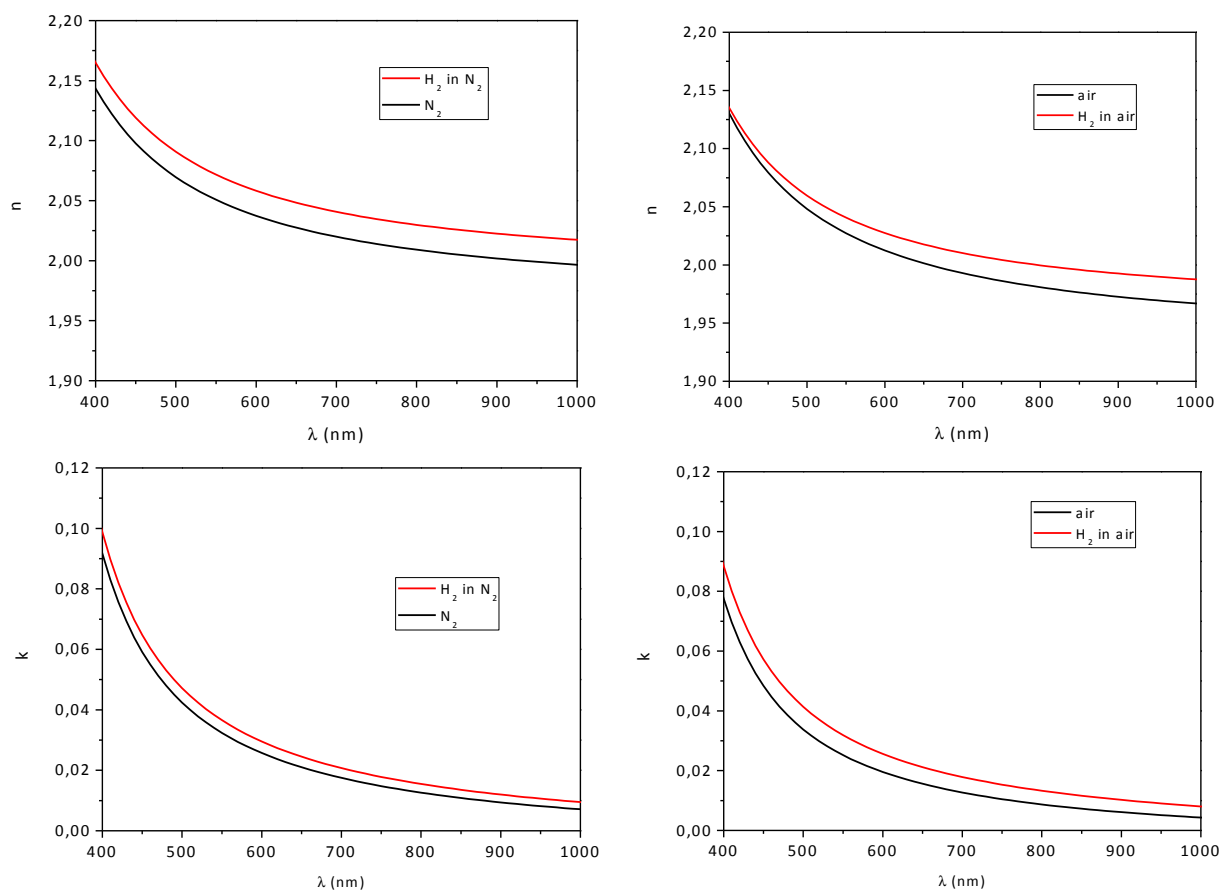
15

Figure S2: Refractive index (n) and extinction coefficient (k) of TiO$_2$ film in N$_2$ and in H$_2$ balanced with N$_2$ (a) and in air and in H$_2$ balanced with air (b).

Publications:
The major part of this work will be submitted as:

1. M. Cittadini, S. Collins, A. Martiucci, P. Mulvaney "Hydrogen Interaction with Single Gold Nanocrystals - A Surface Plasmon Spectroscopy Study" J. Phys. Chem., to be submitted in May 2014.

2. M. Chirea, S. Collins, X. Wei and P. Mulvaney, "Spectroelectrochemistry of Silver Deposition onto Single Gold Nanocrystals", J. Amer. Chem. Soc. (to be submitted May, 2014).

3. PI Mulvaney presented some of this work at an invied talk at the ACS Conference in Dallas in March 2014 and also to groups at University of San Antonio, TX.

Distribution A: Approved for public release. Distribution is unlimited.